PNAS Nexus, 2023, 2, 1–14
https://doi.org/10.1093/pnasnexus/pgad351
Advance access publication 8 November 2023
Research Report

Rhomboid protease RHBDL4/RHBDD1 cleaves SREBP-1c at endoplasmic reticulum monitoring and regulating fatty acids

Song-Iee Han[a,b,1], Masanori Nakakuki[c,1], Yoshimi Nakagawa[a,d], Yunong Wang[a], Masaya Araki[a], Yuta Yamamoto[e], Hiroaki Tokiwa[f], Hiroyuki Takeda[g], Yuhei Mizunoe[a], Kaori Motomura[a], Hiroshi Ohno[a], Kenta Kainoh[a], Yuki Murayama[a], Yuichi Aita[a], Yoshinori Takeuchi[a], Yoshinori Osaki[a], Takafumi Miyamoto[a,h], Motohiro Sekiya[a], Takashi Matsuzaka[a,h], Naoya Yahagi[a], Hirohito Sone[i], Hiroaki Daitoku[j], Ryuichiro Sato[k], Hiroyuki Kawano[c] and Hitoshi Shimano[a,b,j,l,*]

[a]Department of Endocrinology and Metabolism, Institute of Medicine, University of Tsukuba, Tsukuba, Ibaraki 305-8575, Japan
[b]International Institute for Integrative Sleep Medicine (WPI-IIIS), University of Tsukuba, Tsukuba, Ibaraki 305-8575, Japan
[c]Pharmaceutical Research Center, Mochida Pharmaceutical Co., Ltd., Gotemba, Shizuoka 412-8524, Japan
[d]Division of Complex Biosystem Research, Department of Research and Development, Institute of Natural Medicine, University of Toyama, Toyama, Toyama 930-0194, Japan
[e]Department of Chemistry, Rikkyo University, Toshima-ku, Tokyo 171-8501, Japan
[f]Laboratory of Organic Chemistry, Gifu Pharmaceutical University, Daigaku-Nishi, Gifu 501-1196, Japan
[g]Division of Proteo Drug Discovery Sciences, Proteo-Science Center, Ehime University, Matsuyama, Ehime 790-8577, Japan
[h]Transborder Medical Research Center, University of Tsukuba, Tsukuba, Ibaraki 305-8577, Japan
[i]Department of Internal Medicine, Faculty of Medicine, Niigata University, Niigata, Niigata 951-8510, Japan
[j]Life Science Center for Survival Dynamics, Tsukuba Advanced Research Alliance (TARA), University of Tsukuba, Tsukuba, Ibaraki 305-8577, Japan
[k]Department of Applied Biological Chemistry, Graduate School of Agricultural and Life Sciences, Nutri-Life Science Laboratory, The University of Tokyo, Tokyo 113-8657, Japan
[l]Japan Agency for Medical Research and Development, Core Research for Evolutional Science and Technology (AMED-CREST), Chiyoda-ku, Tokyo 100-0004, Japan
*To whom correspondence should be addressed: Email: hshimano@md.tsukuba.ac.jp
[1]S.-I.H. and M.N. contributed equally to this work.
Edited By: J. Silvio Gutkind

Abstract

The endoplasmic reticulum (ER)–embedded transcription factors, sterol regulatory element-binding proteins (SREBPs), master regulators of lipid biosynthesis, are transported to the Golgi for proteolytic activation to tune cellular cholesterol levels and regulate lipogenesis. However, mechanisms by which the cell responds to the levels of saturated or unsaturated fatty acids remain underexplored. Here, we show that RHBDL4/RHBDD1, a rhomboid family protease, directly cleaves SREBP-1c at the ER. The p97/VCP, AAA-ATPase complex then acts as an auxiliary segregase to extract the remaining ER-embedded fragment of SREBP-1c. Importantly, the enzymatic activity of RHBDL4 is enhanced by saturated fatty acids (SFAs) but inhibited by polyunsaturated fatty acids (PUFAs). Genetic deletion of RHBDL4 in mice fed on a Western diet enriched in SFAs and cholesterol prevented SREBP-1c from inducing genes for lipogenesis, particularly for synthesis and incorporation of PUFAs, and secretion of lipoproteins. The RHBDL4-SREBP-1c pathway reveals a regulatory system for monitoring fatty acid composition and maintaining cellular lipid homeostasis.

Keywords: SREBP-1c, RHBDL4, PUFA, p97/VCP

Significance Statement

It is well known that the cleavage system of sterol regulatory element-binding proteins (SREBPs) is sterol-regulated by SREBP-cleavage-activating proteins (SCAP) and insulin-induced gene (Insig) proteins. However, the regulatory mechanism of SREBP-1c by fatty acids is still poorly understood. In this study, we identified RHBDL4/RHBDD1, a member of the rhomboid protease family, as a key cleavage enzyme of SREBP-1c at the endoplasmic reticulum. RHBDL4 shows different activities on SREBP-1c cleavage depending on the type of fatty acids. Our findings elucidated how lipogenesis is nutritionally and differentially regulated by saturated and polyunsaturated fatty acids. The RHBDL4-SREBP-1c pathway represents a unique type of regulated intramembranous proteolysis.

Competing Interest: The authors declare no competing interest.
Received: August 27, 2023. **Accepted:** October 2, 2023

Introduction

Sterol regulatory element-binding protein-1a, -1c, and -2 (SREBP-1a, -1c, and -2) are a transcription factor family that regulate the biosynthesis and uptake of lipids (1, 2). SREBP-1a regulates the production of phospholipids, fatty acids, and cholesterol, providing the entire repertoire of membrane lipids for cell proliferation. SREBP-1c is involved in the synthesis of fatty acids and triglycerides (TGs) in liver and adipose tissues. SREBP-2 acts as the master regulator to maintain cholesterol levels, controlling the expression of the full set of cholesterol synthesis–related genes and the low-density lipoprotein receptor (LDLR) gene, in response to the demands on cellular sterols (3–5). SREBP-1c and SREBP-2 have contrasting activation mechanisms. SREBP-1c activation is mainly thought to be regulated transcriptionally, which is dependent on the intake of carbohydrates or elevated insulin. In contrast, SREBP-2 activation is regulated posttranslationally through proteolytic cleavage system in the cytoplasm (1, 2). The SREBP protein is located as a precursor form in the endoplasmic reticulum (ER) membrane and nuclear envelope. To fulfill the transcriptional role of SREBP in nucleus, it needs to depart from the ER membrane, following the proteolytic cleavage of SREBP. The proteolytic processes are mainly regulated by the levels of cholesterol and its sterol derivatives in the cell, particularly in the ER. Upon sterol deprivation, SREBP precursor moves from the ER and shifts to the Golgi apparatus by escort of the sterol-sensor protein, SREBP-cleavage-activating protein (SCAP). Subsequently, SREBP receives two steps of intramembrane proteolysis by site-1 protease (S1P) and site-2 protease (S2P) located in the Golgi membrane. The released N-terminal fragment of SREBP is transported to the nucleus by importin beta. If cellular cholesterol is abundant, the ER-retaining protein, insulin-induced genes (Insigs), interacts with the SREBP–SCAP complex and prevents their shift to the Golgi apparatus. Thus, the proteolytic cleavage of SREBP-2 is strictly regulated by this sterol-dependent system to maintain cholesterol homeostasis (6).

The proteolytic process for activation of SREBP-1c is somewhat a different feature from that of SREBP-2. The SREBP-1c processing system is influenced by various factors, such as insulin, carbohydrates, and polyunsaturated fatty acids (PUFAs), in addition to sterols (7). PUFAs show obvious inhibitory effect on the proteolytic process of SREBP-1 but has much less effect on SREBP-2 (8). Based on the difference in selectivity of PUFA between SREBP isoforms, we hypothesized that an alternative pathway for SREBP-1c activation may exist, which is independent from the proteolysis by S1P and S2P. Using mutant SREBPs in which the known cleavage sites of SREBP are disrupted by introducing alanine point mutations into the S1P, S2P, and caspase 3 (CPP32) sites, we previously showed that mutant SREBP-2 was incapable of generating the nuclear form but that the corresponding mutant of SREBP-1c retained the potential to produce its nuclear form (9). We observed that this proteolytic process of mutant SREBP-1c was still suppressed by eicosapentaenoic acid (EPA). From these differences in cleavage modes of SREBP-2 and -1c, we suspected that control of SREBP-1 may be dictated by unknown proteases sensitive to PUFAs (9). Furthermore, using the antibiotic Brefeldin A as an inhibitor of the transport of ER proteins to the Golgi and various protease inhibitors as tools, it was shown that this alternative process of SREBP-1c occurs at the ER by serine protease(s) probably without shifting to the Golgi (9).

In an attempt to seek for the responsible enzyme, we remark the rhomboid proteases from the protease group of regulated intramembrane proteolysis (RIP), in which S2P is also included (10). The rhomboid family match the conditions in that the members are intramembrane serine proteases and cleave the intramembrane helices of substrates, and these activities are regulated by phospholipid environments in the cell membrane (11, 12). In human, five enzymatically active rhomboid proteases are known: RHBDL1, RHBDL2, RHBDL3, RHBDL4, and PARL. Among them, RHBDL4 was assumed to be promising candidate that resides in the ER membrane (11, 12). In this study, we found that RHBDL4 is responsible for the proteolytic cleavage of SREBP-1c under PUFA regulation and that this pathway is involved in lipogenic genes regulated by fatty acids.

Results

RHBDL4 cleaves precursor SREBP-1c in a fashion independent of SCAP-Insig system

To identify the unknown enzyme responsible for PUFA-regulated cleavage of SREBP-1c (Fig. 1A), we surveyed serine proteases associated with RIP, based upon our previous results (9). We comprehensively screened mammalian rhomboid proteases. The precursor form of human SREBP-1c tagged at the N-terminus with HSV epitope tag was transfected into HEK293 cells along with the five human rhomboid proteases. By western blot (WB) analysis using an antibody to the HSV tag, production of the short forms of SREBP-1c was examined in nuclear extracts (NE) to test whether any of those enzymes might cleave SREBP-1c and generate the nuclear fragment. Only RHBDL4 cleaved SREBP-1c as compared with empty vector controls (Fig. 1B). Transfection of RHBDL4 also enhanced cleavage of SREBP-1a and -2 that runs at slower mobility than SREBP-1c in NE (Fig. S1A and B). To specifically evaluate the effect of RHBDL4 on SREBP-1c cleavage and resultant nuclear translocation and transactivation, the Gal4-VP16 luciferase assay system was used. In this system, the expression of SREBP-1c and -2 fusion protein exhibited a modest basal luciferase activity that was robustly enhanced by overexpression of RHBDL4 (Fig. S1C). The serine residue at 144 amino acid in RHBDL4 is critical for its protease activity on other substrates, such as the α chain of the pre-T cell receptor (pTα) (13, 14). The catalytically dead mutant, RHBDL4 S144A, attenuated the production of cleaved SREBP-1c in NE (Fig. 1C), indicating that this residue is critical for cleavage of SREBP-1c. Consistent as the sterol-regulated SREBP-cleavage system, SCAP overexpression increased nuclear SREBP-1c protein, and additional coexpression of Insig1 suppressed the SCAP-enhanced SREBP-1c cleavage (Fig. 1D). Strikingly, RHBDL4-induced SREBP-1c cleavage resulted in more pronounced accumulation of nuclear SREBP-1c compared with SCAP. RHBDL4 products from SREBP-1c were broad, containing a part migrating more slowly than that from SCAP induction, suggesting that the RHBDL4-induced cleavage of SREBP-1c may occur at multiple sites proximal to the cleavage site by S2P (Fig. 1D). In contrast, Insig1 did not affect RHBDL4-induced SREBP-1c cleavage (Fig. 1D). Next, we compared the effects of RHBDL4 and SCAP on a 3 M mutant which entirely prevents sterol-regulated and apoptosis-induced cleavages (9). The increase of nuclear SREBP-1c protein after SCAP overexpression observed for the wild type (WT) was completely abrogated by replacement with the 3 M mutant SREBP-1c. Importantly, RHBDL4 exhibited similarly strong activation of cleavages for both WT and 3 M mutant SREBP-1c, indicating that the cleavage by RHBDL4 occurs at different site(s) from those for S1P, S2P, and CPP32 (Fig. 1E). To examine whether cleavage of SREBP-1c by RHBDL4 is independent of the SCAP system, we investigated RHBDL4-mediated SREBP-1c

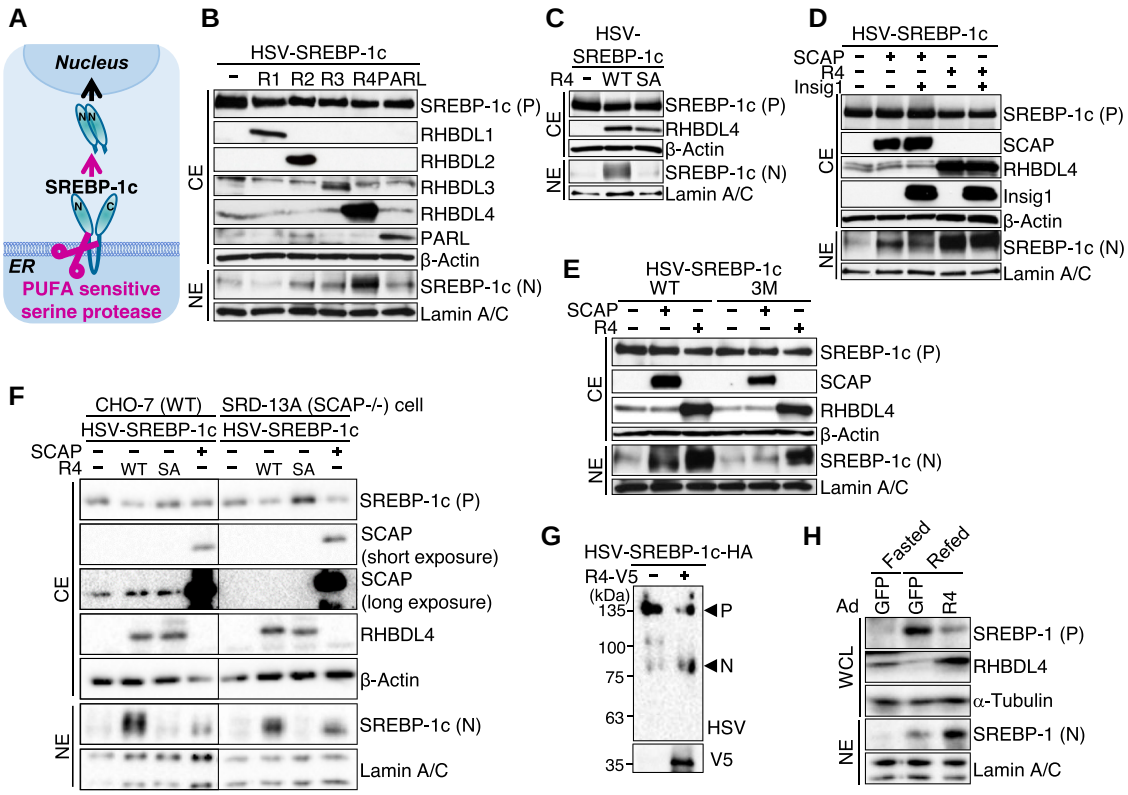

Fig. 1. RHBDL4 cleaves SREBP-1c independently of the SCAP-Insig system. A) Schematic diagram of SREBP-1c cleavage by PUFA-sensitive serine protease on the ER membrane. B–F) Indicated proteins were transiently transfected into HEK293 cells (B–E) or CHO-7 and SRD-13A (SCAP−/−) cells (F). After 24 h, cytosolic extracts (CE) and NE were immunoblotted with the indicated antibodies. SREBP-1c cleavage by rhomboid protease family (B), SREBP-1c cleavage by RHBDL4 mutant S144A (C), SREBP-1c cleavage after coexpression of RHBDL4 and Insig1 (D), SREBP-1c mutant 3 M cleavage by RHBDL4 (E), and SREBP-1c cleavage by RHBDL4 in SCAP null cells (F) are shown. HSV-SREBPs were immunoblotted with HSV antibodies. (-), mock; R1, RHBDL1; R2, RHBDL2; R3, RHBDL3; R4, RHBDL4; WT, wild type; SA, the catalytically inactive mutant of RHBDL4 S144A; 3 M, three known cleavage sites for CPP32, S2P, and S1P mutant of SREBP-1c; P, precursor; N, nuclear. G) An in vitro cleavage assay was performed using recombinant HSV-SREBP-1c-HA and RHBDL4-V5 purified from a cell-free protein synthesis system using wheat germ. Indicated proteins were analyzed by immunoblotting. Arrowheads show precursor (P) and nuclear (N) SREBP-1c. H) Eight-week-old male C57BL/6J mice were injected with GFP- or RHBDL4-expressing adenovirus via the tail vein. Six days after injection, the mice ($n = 3$–4 per group) were subjected to fasting and refeeding. Immunoblot analysis of indicated proteins in whole cell lysates (WCL) and NE from pooled mouse livers was performed.

cleavage in SRD-13A (SCAP−/−) cells lacking SCAP. HSV-tagged SREBP-1c along with RHBDL4, RHBDL4 S144A, or SCAP was coexpressed in CHO-7 (WT) and SRD-13A cells, and then, nuclear SREBP-1c cleavage was tested by WB analysis. In CHO-7 cells, as well as SCAP, RHBDL4 exhibited robust cleavage of SREBP-1c, which was canceled by the RHBDL4 S144A (Fig. 1F). Importantly, cleavage of SREBP-1c by RHBDL4 was also clearly observed in SRD-13A cells but not by the RHBDL4 S144A. These results indicate that cleavage of SREBP-1c by RHBDL4 is independent of the presence or absence of SCAP. We also examined whether SREBP-1c cleavage by RHBDL4 is independent of S1P and S2P. We transfected HEK293A cells with siRNAs for S1P and/or S2P and examined the cleavage by RHBDL4. The cleavage of SREBP-1c by RHBDL4 was still observed even if S1P or S2P alone or both were knocked down (Fig. S1D and E). In addition, we also examined M19 (S2P−/−) cells lacking S2P. In M19 cells, while the cleavage of SREBP-1c by SCAP was not observed unlike CHO-7 cells, cleavage by RHBDL4 exhibited a pattern similar to that of CHO-7 cells (Fig. S1F). The data clearly showed that cleavage of SREBP-1c by RHBDL4 is also independent of S1P or S2P as well as SCAP. SREBP-2 was also cleaved by RHBDL4 in SRD-13A cells (Fig. S1G). Taken together, RHBDL4 cleaves SREBPs independently via preexisting pathways. Then, we tested whether RHBDL4 is the only requisite for SREBP-1c cleavage. Pure human recombinant SREBP-1c protein and human RHBDL4 WT and S144A protein were prepared using a cell-free protein expression system derived from wheat germ. These proteins were mixed in detergent micelles to evaluate the direct proteolytic activities of RHBDL4 dependent on its catalytic amino acid (Fig. 1G and Fig. S1H). This reconstitution of proteolysis demonstrated that RHBDL4 is able to robustly generate nuclear-sized SREBP-1c from the decreased precursor protein, thereby confirming that RHBDL4 rhomboid activity is sufficient for cleavage of SREBP-1c. Moreover, RHBDL4-induced SREBP-1 cleavage observed in cultured cells was evaluated in mouse livers (Fig. 1H). After adenoviral RHBDL4 infection into mice, hepatic SREBP-1 was investigated in a refed state after fasting, the condition in which endogenous precursor SREBP-1 is strongly induced. This hepatic overexpression of RHBDL4 markedly increased levels of the nuclear form of SREBP-1 protein, indicating that RHBDL4 also cleaves SREBP-1 in vivo.

We investigated the region containing the RHBDL4-mediated cleavage site(s) within SREBP-1c using placental alkaline phosphatase (PLAP)-SREBP-1c chimera proteins (Fig. S2A and B). The data suggest that RHBDL4-mediated cleavage can occur at more than one site: one is in the region near first transmembrane domain (TM1) and the other in C-loop or TM2 (Fig. S2A). Diverse prokaryotic and eukaryotic rhomboid proteases share consensus motifs: a less stringent Arg-$(X)_n$-Arg motif for cleavage of substrate proteins within or the near the membrane domain (15). The corresponding motif (LDRSRL) was also found in SREBP-1c,

overlapping the one for S2P as depicted in Fig. S2C. We made several mutants by amino acid substitution near the TM domain of SREBP-1c and tested their cleavages by RHBDL4 (Fig. S2D). Consistent with PLAP data, two cleaved bands (long and short forms) from WT SREBP-1c were detected. From the mutation analysis of the LDRSRL region, mutation of serine 462 to phenylalanine (S462F) prevented the shorter cleaved form of SREBP-1c, but L459F and L464F substitutions did not.

When this mutation was introduced into the Gal4-VP16 luciferase assay, Gal4-SREBP-1c S462F completely abrogated its basal activity, whereas the marked induction by RHBDL4 overexpression observed in WT Gal4-SREBP-1c was partially reduced (Fig. S2E). The data suggest that both the short and the long forms of RHBDL4-mediated SREBP-1c cleavage contribute to SREBP-1c transactivation in which only the short form was sensitive to S462F mutation and that the basal activity in HEK293A cells might reflect the levels of activity of endogenous RHBDL4. The fact that the long form also possesses the transactivity suggests that RHBDL4 cleaves at the site other than the TM1 region of SREBP-1c to cause a nuclear transport of the embedded product. More detailed identification of the cleavage sites by mass spectrometry or other methods remains to be determined.

The RHBDL4–SREBP-1c complex structure was modeled using the Molecular Operating Environment (MOE) program. As shown in Fig. S2F, the S2P recognition and cleavage site at TM1 in SREBP-1c fits a groove near the catalytic triad site of RHBDL4 (histidine 80, serine 144, and histidine 195) well, consistent with our mutational analysis. These data suggested that the DRSR region is important for substrate recognition and the resultant cleavage by RHBDL4 to the short form of SREBP-1c but that the recognition mode should be different between these two proteases in different organelles. This is consistent with the 3 M mutant that prevents S2P cleavage still being cleaved by RHBDL4.

RHBDL4 and SREBP-1c colocalize and interact at the ER to release a nuclear form of SREBP-1c

RHBDL4 was reported to be located at the ER as an intramembrane protease where membrane-bound SREBP-1c typically resides (13). Reconfirming this, it was demonstrated that RHBDL4 colocalized with an ER marker protein. In addition, costaining of RHBDL4, SREBP-1c, and the ER marker protein Calnexin or the Golgi marker protein GM130 showed that RHBDL4 colocalized with SREBP-1c at the ER. This indicates that SREBP-1c could be a substrate for RHBDL4 directly at the ER without additional ER-to-Golgi trafficking as observed in the SCAP-S1P-S2P system (Fig. 2A). In immunoprecipitation (IP) experiments with coexpressed HSV-tagged SREBP-1c and V5-tagged RHBDL4 in HEK293A cells, the immune-reactive V5-tagged RHBDL4 signal was detected after IP with the HSV tag antibody, indicating the proteins can interact (Fig. 2B). IP experiments also showed an interaction between RHBDL4 and SREBP-2, albeit weaker than the interaction with SREBP-1c (Fig. S2G). Other combinations of complex formation were also examined by reciprocal IP experiments of RHBDL4 as well as further IP experiments with each member of the SREBP–SCAP–Insig complex. V5-tagged RHBDL4 was also immunoprecipitated with both HA-tagged SCAP and Myc-tagged Insig1 (Fig. 2C and D). Validation of these IP experiments was ensured by confirming an interaction of SCAP with both SREBP-1c and Insig1 (Fig. 2E). The data indicated that RHBDL4 physically interacts with SREBP-1c, SCAP, and Insig1, suggesting the possibility that RHBDL4 can form a part of the SREBP-1c–SCAP–Insig complex at the ER, although the two systems work separately.

To assess the consequence of the proteolytic cleavage of SREBP-1c by RHBDL4, the processing of SREBP-1c was visualized and translocation to the nucleus was tested. SREBP-1c doubly labeled with yellow fluorescent protein (YFP) at the N-terminus and with cyan fluorescent protein (CFP) at the C-terminus (YFP-SREBP-1c-CFP) was transfected with mCherry-labeled RHBDL4 or SCAP in HeLa cells, a SREBP abundant cell line. In the absence of SCAP or RHBDL4 overexpression, both YFP- and CFP-SREBP-1c signals were localized and merged in the cytosol assuming to be at the ER according to the data from Fig. 2F. After mCherry-tagged SCAP coexpression, the signal of N-terminal YFP-SREBP-1c shifted to the nucleus, whereas the signal of C-terminal CFP-SREBP-1c remained in the cytosol. After coexpression of mCherry-RHBDL4, the signal of N-terminal YFP-SREBP-1c similarly shifted to the nucleus, indicating transfer of N-terminal SREBP-1c into nucleus. The mCherry-RHBDL4 S144A showed a trend of decrease in the nuclear appearance of SREBP-1c (Fig. 2F), although statistically not significant (Fig. 2G).

We then tested if nuclear translocation also resulted in transactivation of SREBP-1c using a luciferase-based reporter assay with a SREBP binding cis-element (SRE) in the promoter region. Coexpression of the precursor forms of SREBP-1c with either SCAP or RHBDL4 significantly elevated the transcriptional activity, although less strongly after RHBDL4 expression (Fig. 2H). Taken together, these data in cell lines indicate that RHBDL4 overexpression results in N-terminal SREBP-1c cleavage, nuclear translocation, and consequent transcriptional activity.

RHBDL4 siRNA knockdown reduces nuclear SREBP-1 protein and suppresses target gene expression

We hypothesized from control data in our overexpression experiments that there may be a contribution from endogenous RHBDL4. To test the physiological contribution of RHBDL4 to SREBP-1 processing, RHBDL4 knockdown experiments were performed to investigate the effects on the levels of cleaved SREBP-1 protein in NE and its target gene expression in HepG2 and HEK293 cells. Two independent RHBDL4 siRNAs effectively abolished endogenous RHBDL4 protein in both cell lines. We observed that the classical sterol regulation in these cells obscured the effect from endogenous RHBDL4 (Fig. S3A and B). To suppress the endogenous effect mediated from SCAP, 25-hydroxycholesterol was added to inhibit the SCAP-S1P-S2P process. HepG2 and HEK293 cells transfected with RHBDL4 siRNA showed a clear decrease in nuclear SREBP-1 protein levels without any change in precursor levels of SREBP-1 treated with 25-hydroxycholesterol (Fig. S3A and B). Gene expression analysis revealed RHBDL4 siRNA diminished *Rhbdl4* (*Rhbdd1*) mRNA, with a slight concomitant reduction of *Srebp-1* (*Srebf1*) mRNA in HepG2 cells. SREBP-1 target genes, stearoyl-CoA desaturase 1 (*Scd1*), fatty acid desaturase 1 (*Fads1*), and thyroid hormone responsive (*Thrsp*), were all significantly suppressed by both of the two RHBDL4 siRNAs (Fig. S3C). However, neither the decrease in nuclear SREBP-1c protein nor the decrease in expression of downstream target genes by RHBDL4 knockdown was observed when the SCAP system was working without 25-hydroxycholesterol treatment (Fig. S3C). The data indicate that endogenous RHBDL4 is involved in SREBP-1 activation and subsequent gene regulation of its target genes independently from sterol regulation. The RHBDL4 knockdown also reduced the gene expression of *Srebp-2* (*Srebf2*) and its target gene, *Ldlr* (Fig. S3C). In contrast, *S1P* (*Mbtps1*) was up-regulated, implicating both SCAP and RHBDL4 systems

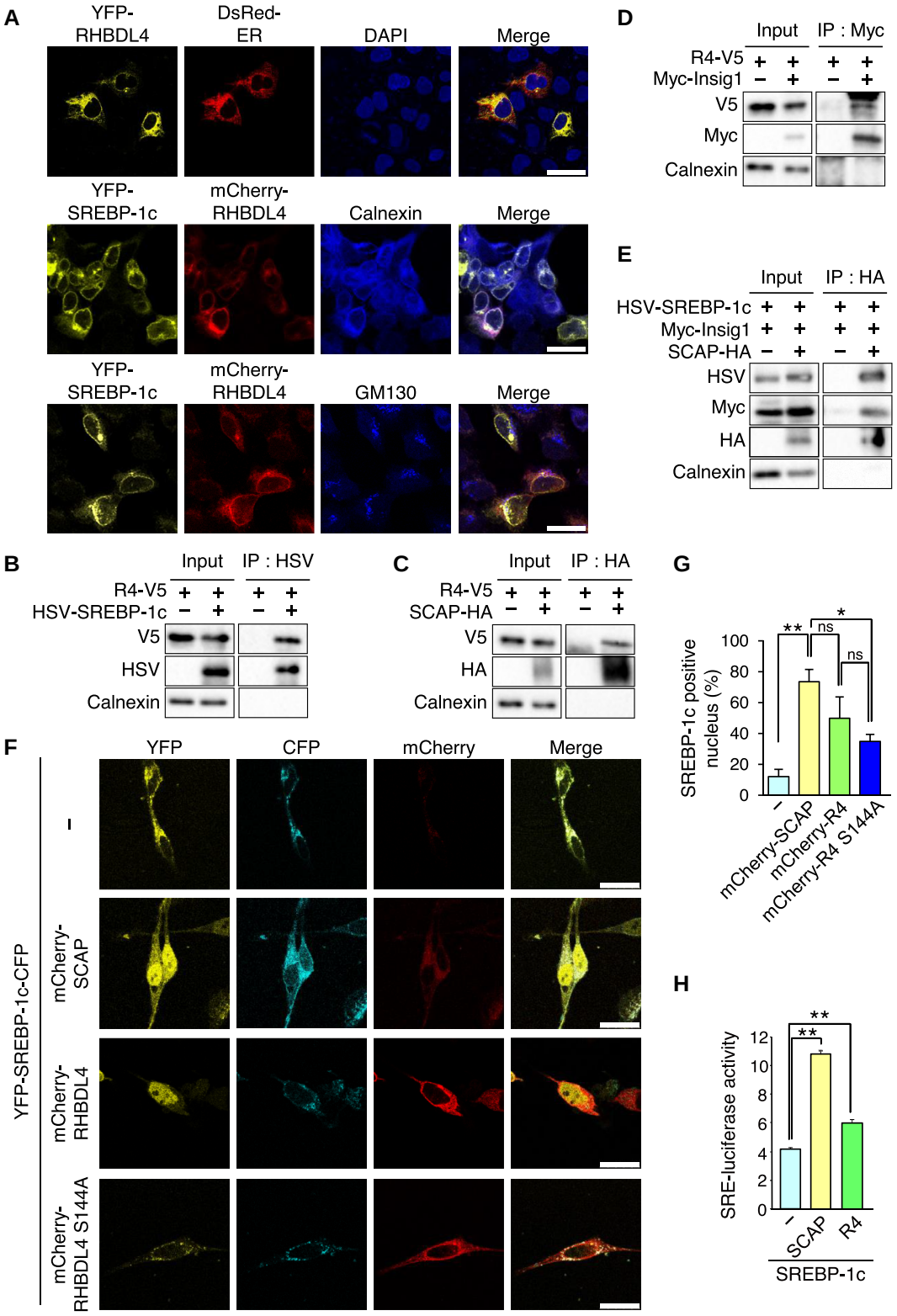

Fig. 2. RHBDL4 interacts with the SREBP-1c–SCAP–Insig complex in the ER and increases nuclear SREBP-1c accumulation. A) Cellular localization of RHBDL4 and SREBP-1c. HEK293A cells expressing the indicated YFP-RHBDL4 and DsRed-ER (top) or YFP-SREBP-1c and mCherry-RHBDL4 (middle and bottom) constructs are shown. Nuclei were stained with DAPI, the ER were stained with Calnexin antibody, and the Golgi were stained with GM130 antibody. Scale bar, 25 μm. B–E) Immunoprecipitation assay. HEK293A cells were transfected with the indicated expression plasmids. After 24 h, cell extracts were immunoprecipitated (IP) with the indicated antibodies. Bound proteins were immunoblotted with the indicated antibodies. Interactions of SREBP-1c and RHBDL4 (B), SCAP and RHBDL4 (C), Insig1 and RHBDL4 (D), and SCAP and SREBP-1c and Insig1 (E) are shown. F, G) Translocation of SREBP-1c to the nucleus by RHBDL4. HeLa cells expressing YFP-SREBP-1c-CFP and mCherry-SCAP, mCherry-RHBDL4, or mCherry-RHBDL4 S144A are shown. Cells with nuclear fluorescence of YFP were counted and the percentages expressed as bar graphs (G). Scale bar represents 25 μm. H) Luciferase assay for SREBP-1c activity. HEK293 cells were transfected with SRE-Luc, pRL-SV40, and the indicated expression plasmids. After 24 h, cell extracts were examined using luciferase assays. Quantification was performed on three (G) or four (H) samples. Data are represented as means ± SEM. $^{*}P < 0.05$; $^{**}P < 0.01$; ns, not significant.

might be coregulated as observed in the obscure data without 25-hydroxycholesterol treatment (Fig. S3C).

RHBDL4 is responsible for activation of hepatic SREBP-1 cleavage and lipogenic gene expression in mice on a Western diet

To clarify the role of RHBDL4 in SREBP-1 cleavage in the liver, RHBDL4 knockout (KO) mice were generated using CRISPR/Cas9. RHBDL4 KO mice were alive and exhibited no apparent anthropometric phenotypes (Fig. S4A and B). On a normal chow diet, the disappearance of hepatic RHBDL4 protein and mRNA was confirmed in the livers of RHBDL4 KO mice, but there were no marked changes in either precursor or nuclear SREBP-1 protein between WT and RHBDL4 KO mice (Fig. 3A and B). The animals were then fed on a Western diet (WD) enriched with cholesterol and SFA for 14 days whereby the precursor form of SREBP-1 in liver was robustly induced due to the gene induction by the LXR-SREBP-1c pathway, resulting in a striking increase in the nuclear form in WT mice. In spite of a similar robust increase in precursor SREBP-1 protein after feeding with a WD, the amount of SREBP-1 protein in NE in RHBDL4 KO mice was strongly reduced (Fig. 3A and Fig. S4C and D). This is indicative of the suppression of SREBP-1 processing in the absence of RHBDL4. RHBDL4 appears to contribute to the cleavage of SREBP-1 in the liver as a response to feeding on a WD. Precursor and nuclear SREBP-2 proteins were not different between the WT and KO mice (Fig. 3A and Fig. S4C and D). We also evaluated the effect of RHBDL4 KO on another SREBP-1c-induced condition: a high-sucrose fat-free (HS) diet. The reduction in nuclear form SREBP-1 from RHBDL4 KO mice was also observed on a HS diet but less prominently when compared with the effects after feeding on a WD (Fig. S4E).

qRT-PCR analysis in mouse livers determined the effects of RHBDL4 disruption on the expression of SREBP target genes (Fig. 3B). *Srebp-1c* (*Srebf1*) gene expression was markedly induced by feeding on a WD, whereas *Srebp-2* (*Srebf2*) gene did not change among the four groups. Hepatic de novo lipogenic genes as SREBP-1 target genes, such as acetyl-CoA carboxylase alpha (*Acaca*), fatty acid synthase (*Fasn*), *Scd1*, ELOVL fatty acid elongase 6 (*Elovl6*), and *Thrsp*, were increased in WT on a WD and markedly suppressed in RHBDL4 KO mice. These changes corresponded to the changes in amounts of nuclear SREBP-1 in the two groups (Fig. 3B). We also examined the expression of ER stress-related genes and found that *Chop* (*Ddit3*) did not change significantly, while *Xbp1s* was increased in WD-loaded KO mice (Fig. S4F). Gene expression for cholesterol synthesis and uptake tended to be decreased by WD for hydroxy-3-methylglutaryl-CoA synthase 1 (*Hmgcs1*) and squalene epoxidase (*Sqle*) genes, with no significant differences between WT and KO. Hydroxy-3-methylglutaryl-CoA reductase (*Hmgcr*) and *Ldlr* were increased by WD and decreased in WD-loaded KO. However, expression of nuclear SREBP-2 did not exhibit significant differences among the four groups, suggesting a regulation mechanism other than SREBP-2 (Fig. 3B). To evaluate the effects of SREBP-2 activation by statin and ezetimibe in RHBDL4 KO mice, we followed a previous paper (16) and treated mice with lovastatin and ezetimibe (S/E) (Fig. S4G and H). WB analysis on livers showed that precursor and nuclear forms of SREBP-2 were increased in both WT and KO mice in the S/E group, while precursor and nuclear forms of SREBP-1 were decreased in S/E-loaded mice, consistent with a previous paper (17). In addition, qRT-PCR results showed that the expression of SREBP-2 and its target genes was significantly increased by S/E, but there was no significant difference between WT and KO. As previously reported (16, 17), gene expression of SREBP-1c was decreased by S/E, while SREBP-1 target genes tended to increase, but no difference was found between WT and KO. These results indicated that RHBDL4 has a specific effect on SREBP-1 activation of lipogenesis rather than SREBP-2 activation of sterol regulation. To further understand the roles of RHBDL4 in the liver from gene expression profiles, livers from RHBDL4 KO and WT mice fed on a normal chow and on a WD were subjected to RNA-seq analysis. The analysis identified 309 genes up-regulated after WD feed compared with the normal chow group, and 85 genes were down-regulated by RHBDL4 KO compared with WT (Fig. 3C). Gene ontology analysis on the 48 overlapping genes resulted in enrichment of SREBP-regulated genes and the LXR pathway, consistent with induction of the LXR-SREBP-1c axis (Fig. 3D). Thus, our identification of RHBDL4 as being responsible for SREBP-1 cleavage and downstream effects on transcription was validated for having an endogenous role in the liver. It is noteworthy that SREBP-1 cleavage by RHBDL4 is prominent only after feeding on a WD.

RHBDL4 directs SREBP-1c activation to PUFA synthesis and remodeling and very-low-density lipoprotein secretion

The genes down-regulated by RHBDL4 KO resulted in similar gene ontology enrichment, suggesting a deep relationship between RHBDL4 and SREBP in lipid metabolism, especially for plasma lipoprotein assembly and remodeling (Fig. 3D). As confirmed by qRT-PCR (Fig. 3E), other gene clusters up-regulated after WD feeding in WT mice but abrogated in RHBDL4 KO mice including genes involved in the incorporation of fatty acids into glycerolipids for the formation of TGs, such as glycerol-3-phosphate acyltransferase (*Gpam*); diacylglycerol O-acyltransferase 2 (*Dgat2*); peroxisome proliferator-activated receptor gamma (*Pparg*); lipid influx–related genes, such as Lipin1 (*Lpin1*); and patatin-like phospholipase domain-containing protein 3 (*Pnpla3*), along with lipoprotein remodeling genes for the secretion of very-low-density lipoprotein (VLDL), such as apolipoprotein A4 (*ApoA4*) (18) and lysophosphatidylcholine acetyltransferase 3 (*Lpcat3*) (19). Changes in these genes suggest that RHBDL4 could be involved in lipid flux between organs via circulation. Genes involved in modification or remodeling of PUFA were also enriched (Fig. 3F): *Elovl2* (20), *Elovl5* (21), *Fads1*, and *Fads2* (22) for the production of long PUFA, *Lpcat3* (23), and 1-acylglycerol-3-phosphate O-acyltransferase 3 (*Agpat3*) (24) for the incorporation of EPA and docosahexaenoic acid (DHA), respectively, into membrane phospholipids. Major facilitator superfamily domain-containing protein 2a (*Mfsd2a*) is a DHA-specific transporter protein showing an outstanding difference by RHBDL4 absence (25–27). These data suggest that RHBDL4 plays a role to maintain membrane PUFA levels counter-balancing lipotoxic stress of SFA and cholesterol by activating these SREBP-1 target genes through the RHBDL4-SREBP-1c and LXR-SREBP-1c pathways. The findings also suggest a potential feedback system between SREBP-1 and PUFA. In terms of physiological relevance, up-regulated gene clusters in RHBDL4 KO mice on a normal chow diet included ER stress- and UPR-related gene pathways, whereas down-regulated genes related to the heat stress response and plasma lipoprotein remodeling (Fig. S4I). In accordance that ER stress was reported after RHBDL4 deletion in cell culture experiments (13), RHBDL4 might be involved in ER membrane stresses through lipid perturbations.

RHBDL4 deletion ameliorates lipid accumulation by WD

The plasma and liver lipids, fatty acid composition, and histological analyses were shown in Fig. 4. Both genotypes after WD

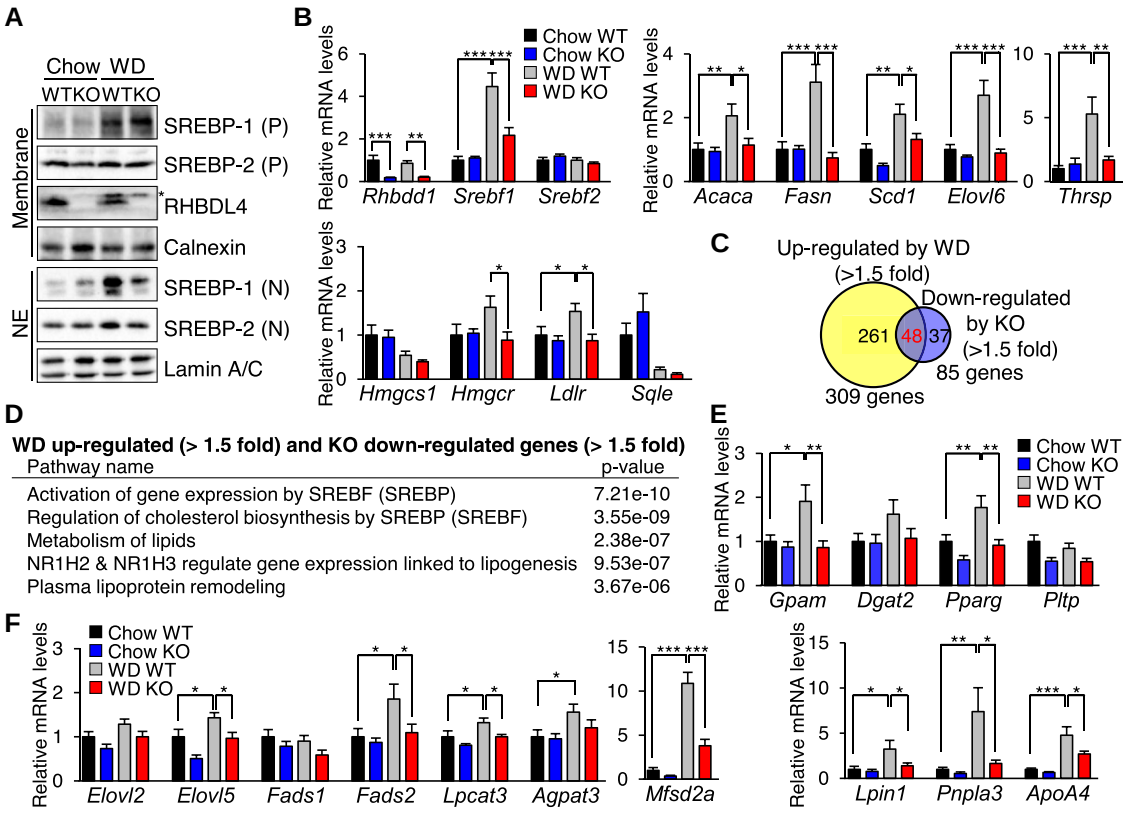

Fig. 3. RHBDL4 contributes to SREBP-1 cleavage and activation in the WD-fed mice. Eight-week-old male WT and RHBDL4 KO mice were fed on normal chow or a WD for 14 days. A) Immunoblot analysis of the indicated proteins in the membrane fraction and NE of pooled mouse livers ($n = 4$ per group). P, precursor; N, nuclear. Asterisk shows nonspecific bands. B) qRT-PCR analysis of lipogenic genes from mouse livers. C, D) RNA-seq analysis of livers of WT and KO mice fed on normal chow or a WD for 14 days (false discovery rate [FDR] < 0.05, $n = 4$). C) Venn diagram of overlap between up-regulated genes from mice fed on a WD (WD induced genes >1.5-fold versus normal chow, top) and down-regulated genes in KO (KO reduced genes >1.5-fold versus WT mice fed on a WD, bottom). D) Functional annotations associated with KO down-regulated genes compared with WT mice fed on a WD and overlapped genes with WD up-regulated genes compared with normal chow. E, F) qRT-PCR analysis of lipoprotein assembly and remodeling genes (E) and PUFA-producing genes (F) in mouse livers. Data are represented as means ± SEM. Quantification was performed on eight samples. *$P < 0.05$; **$P < 0.01$; ***$P < 0.001$.

feeding increased liver and plasma cholesterols and liver TGs. RHBDL4 KO mice showed significantly less plasma and liver TGs than WT mice, consistent with the differences in lipogenic and lipoprotein-related genes in the liver (Fig. 4A). Gas chromatography analysis of the fatty acid composition of liver lipids showed that RHBDL4 KO mice had decreased total fatty acid contents (Fig. 4B). Most individual fatty acids including SFA and PUFA exhibited significant reduction in RHBDL4 KO livers consistent with suppressed lipogenesis. Notably, quantities of arachidonic acid (AA), EPA, docosapentaenoic acid (DPA), and DHA were decreased in RHBDL4 KO mice, consistent with decreased expression of genes required for the incorporation of AA and DHA. On a relative molar% basis, γ-linolenic acid was increased, whereas palmitoleic acid and dihomo-γ-linolenic acid were decreased (Table S1). The ratio of representative ω3 PUFA to ω6 PUFA was also reduced, indicating a trend of proinflammation. Liver histology from hematoxylin and eosin (H&E) staining indicated no marked changes in RHBDL4 KO mice compared with WT on a normal chow (Fig. 4C). As shown in Oil red O (ORO) staining, feeding on a WD caused hepatosteatosis in both genotypes with amelioration of the size and the number of lipid droplets in RHBDL4 KO mice especially in central vein areas compared with WT (Fig. 4D).

PUFA inhibits and SFA activates RHBDL4-dependent SREBP-1c cleavage

It is well known that hepatic SREBP-1c and target lipogenic genes are suppressed by dietary PUFA (8, 28, 29), but the precise molecular mechanism is enigmatic. We investigated this in RHBDL4 KO mice (Fig. 5A and B and Fig. S5A and B). One single day addition of EPA, a representative PUFA on the last day of 14 days WD feeding, caused marked suppression of the nuclear SREBP-1 protein in WT livers as previously reported (28, 29) (Fig. 5A). In contrast, in RHBDL4 KO mice on a WD, the nuclear SREBP-1 amount was already reduced, and only marginal further inhibition was observed with EPA. This suggested that RHBDL4 is partially responsible for EPA-regulated SREBP-1 cleavage. The expression profile of SREBP-1 target genes on an EPA-containing diet is shown (Fig. 5B). As previously reported, *Srebp-1c* (*Srebf1*) expression exhibited a robust reduction by EPA, whereas *Srebp-2* (*Srebf2*) reduction was weak (8). Lipogenic genes of SREBP-1 targets, such as *Fasn*, *Scd1*, and *Elovl6*, were similarly reduced in RHBDL4 KO mice on WD feeding but underwent no further suppression after EPA supplementation, indicating that the substrate cleavage ability by RHBDL4 on SREBP-1 was prevented by EPA feeding. Inhibition of these lipogenic genes by EPA was strongly observed in WT mice but was diminished in RHBDL4 KO mice. The data can be interpreted that a long known suppression of SREBP-1c and lipogenic genes by PUFA was at least partially attributed to RHBDL4 cleavage activity for SREBP-1c. Expression of SREBP-2 downstream target genes, such as *Hmgcs1* and *Hmgcr*, did not show changes between WT and RHBDL4 KO mice irrespective of EPA addition.

In vivo, dietary PUFA suppresses hepatic SREBP-1c mRNA expression and reduces the precursor protein levels. This confounds

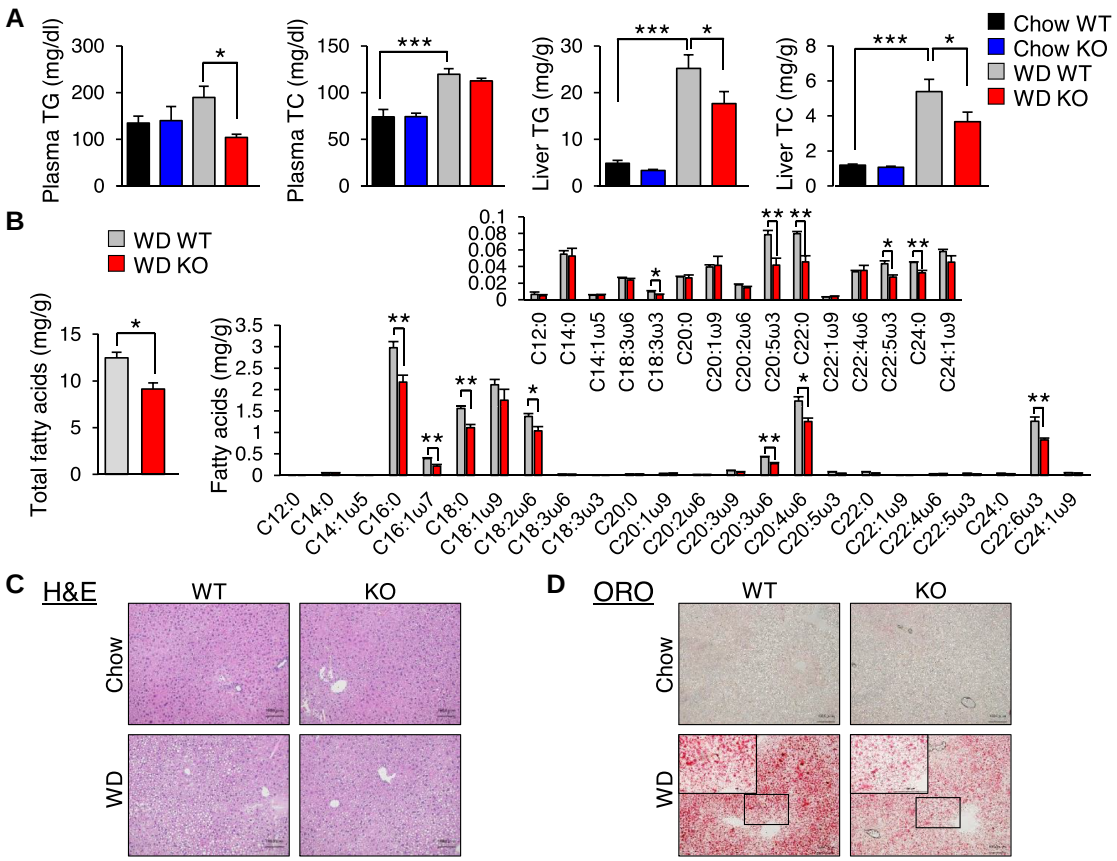

Fig. 4. RHBDL4 deletion reduces lipid accumulation by WD. Eight-week-old male WT and RHBDL4 KO mice were fed normal chow or a WD for 14 days. A) Plasma triglyceride (TG), plasma cholesterol (TC) levels, liver TG, and liver TC contents of mice. Data are represented as means ± SEM. Quantification was performed on eight samples. *$P < 0.05$; ***$P < 0.001$. B) Total fatty acids (left) and fatty acid composition (right) of liver tissue in WT and KO fed a WD for 14 days. Data are represented as means ± SEM. Quantification was performed on four samples. *$P < 0.05$; **$P < 0.01$. C, D) Representative H&E-stained section (C) and ORO-stained section (D) of mouse livers. Scale bar represents 100 μm.

any attempt to estimate PUFA inhibition on SREBP-1 cleavage directly. Instead, we investigated the effect of supplementing various fatty acids to the medium at different concentrations on RHBDL4-dependent SREBP-1c cleavage in HEK293 cells by WB analysis under fixed overexpression of both SREBP-1c and RHBDL4. Figure 5C shows that AA, EPA, and DHA representative PUFAs all inhibit the induction of cleaved SREBP-1c by RHBDL4 in a dose-dependent manner without affecting the level of RHBDL4 protein. Effects of other various fatty acids were also tested (Fig. S5C and D). Most unsaturated fatty acids showed dose-dependent inhibition, whereas palmitic acid (PA) as a representative SFA did not inhibit at these tested concentrations. In contrast to no effect at lower concentrations in Fig. S5C, PA at the concentrations of 50 μM or higher showed marked dose-dependent escalation of the RHBDL4-induced cleavage of SREBP-1c (Fig. 5D). EPA (10 μM) efficiently reversed the agonistic effect of PA (100 μM) (Fig. 5E). IP analysis exhibited that EPA treatment did not affect the interaction between RHBDL4 and SREBP-1c, suggesting that EPA did not affect accessibility of RHBDL4 to SREBP-1c (Fig. S5E). To examine whether fatty acid–induced ER stress is involved in the cleavage of SREBP-1c, we investigated a WB analysis using the ER stress markers XBP1s and CHOP antibodies. The results showed that there were no significant changes in the protein levels of XBP1s and CHOP under the experimental conditions of the present study (Fig. S5F). We also investigated effect of EPA on pTα and myelin protein Z (MPZ) L170R that were reported to be cleaved by RHBDL4 (13). EPA also exhibited suppressive effects on RHBDL4 cleavage activities for these known substrates, which suggested EPA inhibition of the substrate cleavage ability by RHBDL4 is not specific to SREBP-1c (Fig. S5G and H). These results suggest that the balance of fatty acid saturation potentially presumably at the ER membrane is likely to be an important factor for the regulation of the substrate cleavage ability by RHBDL4. RHBDL4 may thereby be involved in ER membrane stresses through sensing and regulating the degree of fatty acid saturation.

RHBDL4-mediated SREBP-1c activation engages p97/VCP–UFD1L–NPLOC4 complex

RHBDL4 has been reported to be involved in the ubiquitin-dependent ER-associated protein degradation (ERAD) of single-spanning and polytopic membrane proteins together with the ternary complex containing p97/valosin-containing protein (VCP), UFD1L, and NPLOC4 (30, 31). This complex might involve dislocation of RHBDL4 substrates from the membrane into cytosol after cleavage. To evaluate whether these factors affect RHBDL4-mediated SREBP-1c activity, the Gal4-VP16 luciferase assay was performed. The addition of p97, UFD1L, and/or NPLOC4 additively enhanced luciferase activity as compared with RHBDL4 alone (Fig. 6A and C). It should be noticed that the auxiliary effects of these factors were negligible without RHBDL4, indicating a functional association with RHBDL4-mediated SREBP activation (Fig. 6B). Other potential modifying factors were also tested: Ubxd8 as a PUFA acceptor and UBA domain-containing 2 (UBAC2) that belongs to the pseudo-rhomboid family lacking

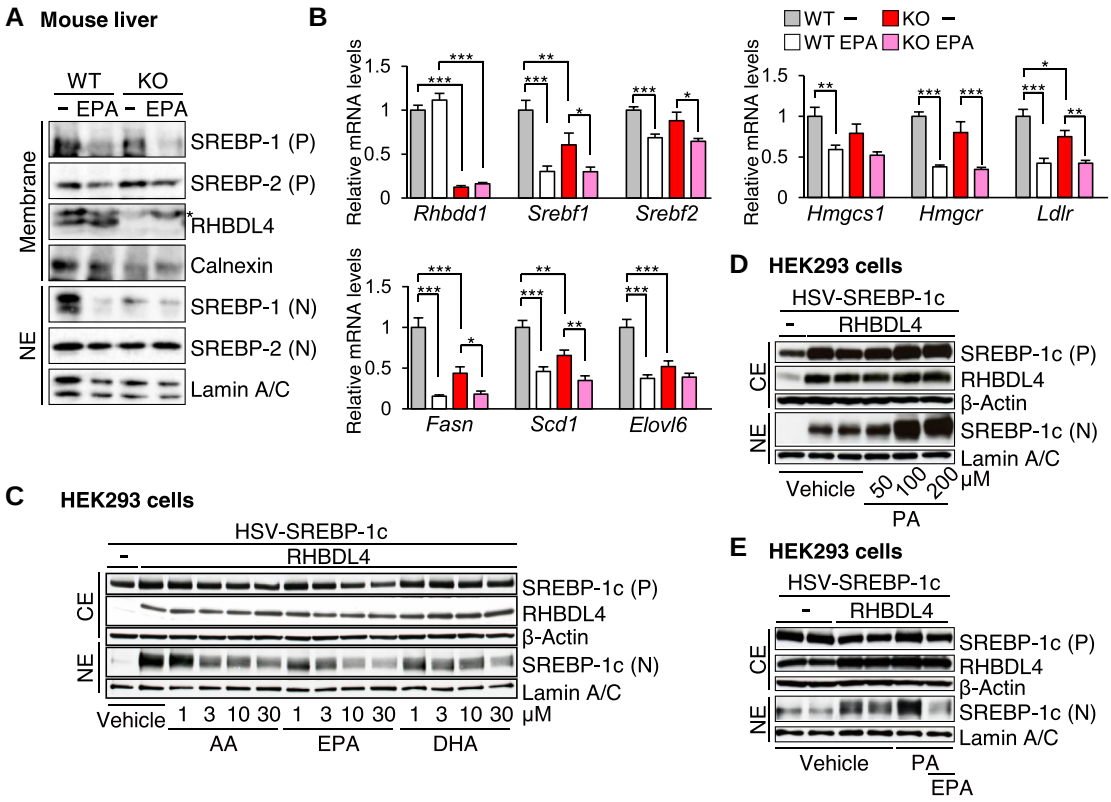

Fig. 5. PUFA inhibits and SFA activates RHBDL4-dependent SREBP-1c cleavage. A, B) Eight-week-old male WT and RHBDL4 KO mice were fed a WD for 14 days and treated with 5% EPA-E once the last day. A) Immunoblot analysis of indicated proteins in the membrane fraction and NE of pooled mouse livers ($n = 2$ per group). P, precursor; N, nuclear. Asterisk shows nonspecific bands. B) qRT-PCR analysis of lipogenic genes in mouse livers. Data represented as means ± SEM. Quantification was performed on 9–10 samples. $^{*}P < 0.05$; $^{**}P < 0.01$; $^{***}P < 0.001$. C–E) HEK293 cells were transfected with HSV-SREBP-1c and RHBDL4 expression plasmids. After 4 h, cells were incubated with 10% delipidated serum (DLS) containing the indicated concentration of each fatty acid for 20 h. Immunoblot analysis of the indicated proteins in CE and NE was performed. SREBP-1c cleavage by AA, EPA, and DHA (C), SREBP-1c cleavage by PA (D), and SREBP-1c cleavage by 100 μM PA and 10 μM EPA (E) are shown. P, precursor; N, nuclear.

protease activity (32, 33). Although Ubxd8 did not affect SREBP-1c cleavage activity, UBAC2 robustly inhibited RHBDL4-p97-mediated SREBP-1c activation (Fig. 6D). Inhibition of RHBDL4-dependent SREBP-1c cleavage by PUFA shown in Fig. 5 was completely recaptured in this reporter assay (Fig. 6E). EPA suppression was minimal in the absence of RHBDL4, supporting the hypothesis that PUFA mediates the regulation of SREBP-1c cleavage via RHBDL4 (Fig. 6E).

To explore the function of p97, UFD1L, and NPLOC4 on an endogenous basis, individual siRNAs were used in HepG2 cells. Effective knocking-down by each of the three factor siRNAs was confirmed at both mRNA and protein levels (Fig. 6F and G). NPLOC4 siRNA was found to suppress UFD1L protein level completely without affecting its mRNA level, suggesting that NPLOC4 is required for UFD1L stability (Fig. 6F). Results showed that SREBP-1 protein in NE from the cleavage ability by RHBDL4 was considerably reduced by p97 siRNA and UFD1L siRNA but not by NPLOC4 siRNA. Precursor SREBP-1 and RHBDL4 proteins detected in the cytosolic fraction were not changed by any of the tested siRNAs, indicating the effects on SREBP-1 cleavage. As for the effects on SREBP-1 target genes, p97, UFD1L, and NPLOC4 siRNAs caused a decrease in *Scd1*, *Fads1*, and *Thrsp* (Fig. 6G). These data suggest that UFD1L and NPLOC4 may regulate the expression of SREBP-1c-targeted lipid synthesis genes by a pathway that does not directly involve cleavage of SREBP-1c by RHBDL4. p97 siRNA induced *Srebp-1* (*Srebf1*) expression (Fig. 6G), whereas p97, UFD1L, and NPLOC4 siRNAs induced *Rhbdl4* (*Rhbdd1*) and *S1P* (*Mbtps1*) expression and suppressed *Insig1* and *Insig2* expression, further supporting adaptive regulation between the RHBDL4 system and SCAP system (Fig. 6G and Fig. S6A).

An auxiliary role of p97 was investigated in the context of short and long forms of RHBDL4-mediated SREBP-1c cleavage and activation (Fig. S6B). The decreased, but still remnant, activity in S462F SREBP-1c by RHBDL4 (Fig. S1F) was enhanced by p97 to a similar extent to wild SREBP-1c, whereas the decrease by S462F was not changed by p97, indicating that p97 enhancement is specific to the longer membrane embedded form. These data suggest that the effect of p97 on RHDBL4 cleavage might be related to its segregase activity in extracting the longer cleaved SREBP-1c out of ER membranes. Roles of the versatile factor p97 in lipid metabolism are not fully understood and are the target of future studies. ERAD is likely to be involved, since RHBDL4 that carry a mutation of the ubiquitin interaction motif show decreased cleavage activity for SREBP-1c (Fig. S6C).

Discussion

The current study demonstrated that rhomboid protease RHBDL4, a membrane-bound serine protease, directly cleaves SREBP-1c at the ER. This is consistent with previous data indicating that Rbd2, the Golgi yeast rhomboid homolog, cleaves Sre1, the SREBP homolog in yeast that is important for the response to hypoxia at the Golgi (34, 35). Our data highlight that RHBDL4 at the ER or nuclear envelope is regulated by fatty acids. PUFA and monounsaturated fatty acid (MUFA) are inhibitory, whereas SFA act to enhance the substrate cleavage ability by RHBDL4. In a series of

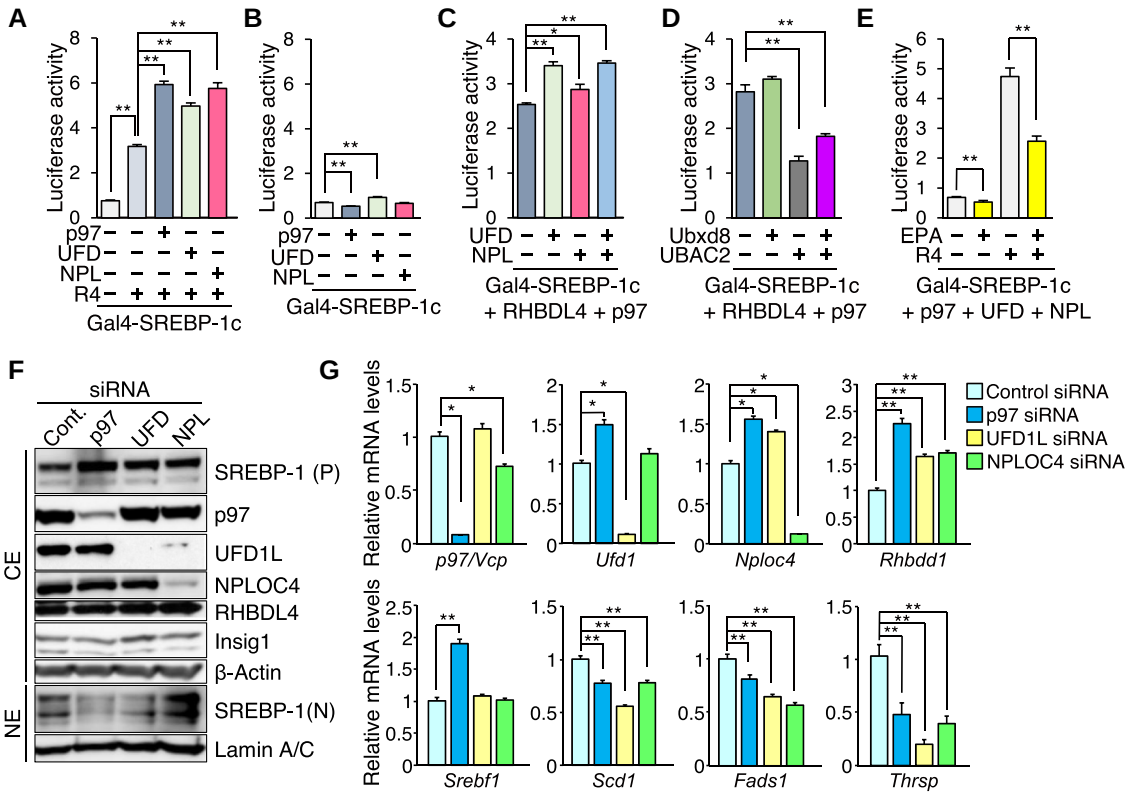

Fig. 6. AAA-ATPase p97 supports RHBDL4-induced SREBP-1c activation. A–E) Luciferase assay of SREBP-1c activity by AAA-ATPase p97. HEK293 cells were transfected with Gal4-RE-Luc, pRL-SV40, and the indicated expression plasmids. After transfection, cells were treated with 50 μM EPA (E). After 24 h, cell extracts were examined using luciferase assays. Quantification was performed on four samples. F, G) HepG2 cells were transfected with the indicated siRNA. After 24 h transfection, cells were incubated with 10% DLS containing 3 μM 25-hydroxycholesterol for 24 h. F) Immunoblot analysis of the indicated proteins in CE and NE. Cont., control; P, precursor; N, nuclear. G) qRT-PCR analysis of SREBP-1 and related genes was performed. Quantification was performed on six samples. Data are represented as means ± SEM. $^{*}P < 0.05$; $^{**}P < 0.01$.

both in vitro and in vivo experiments, we confirmed that RHBDL4 is responsible for a PUFA-regulated SREBP-1c cleavage system and comprise a hepatic SREBP-1c-lipogenesis pathway that is regulated by feeding on a WD and by dietary PUFA. Since RHBDL4 has been recognized as a part of ERAD system, our findings that RHBDL4 induces nuclear SREBP-1c proteins on lipotoxic conditions need to be interpreted under this system in lipid-rich and, thus, ER stress-prone conditions, which requires further investigation including ubiquitination of SREBPs.

The process for the cleavage and transactivation of SREBP, especially SREBP-2, is tightly controlled. This occurs mediated through the cholesterol-sensing complex of SREBP2–SCAP–Insigs on the ER as the main machinery for cholesterol feedback regulation, which has been intensively analyzed and revealed by the Goldstein and Brown group. In contrast, SREBP-1c is involved in lipogenesis regulated nutritionally. Nuclear SREBP-1c activity is strongly enhanced by cholesterol and SFA intakes. However, SREBP-1c is also supposed to bind to SCAP-Insigs and, thus, cannot transfer to the Golgi apparatus for cleavage by S1P and S2P in those lipotoxic conditions. In this study, we elucidated this paradox by RHBDL4 (Fig. 7). Retaining at the ER in cholesterol abundance, N-terminal domain of SREBP-1c can be then cleaved by RHBDL4 activated in SFA abundance for nuclear transport. For gene induction, RHBDL4 prefers SREBP-1c-mediated lipogenesis to SREBP-2-mediated cholesterol synthesis. In the cell culture experiments, RHBDL4 is molecularly able to cleave and execute nuclear transport for both SREBP-1c and SREBP-2 proteins. In vivo, detailed distinctive roles of RHBDL4 on the two isoforms of SREBPs regulated by PUFA, SFA, and cholesterol along with mutual interaction with SCAP-Insig-SREBP system are a future consideration.

Our data indicate that there are different (short and long) fragments after RHBDL4 cleavage. Once cleaved near TM1, the short form can be released into the nucleus (Fig. 7). Another cleaved product (long fragment) is likely to be still embedded in the ER membrane and requires another step for nuclear translocation (Fig. 7). We propose that the p97–UFD1L–NPLOC4 complex facilitates this process by extracting the ER membrane–stacking fragment. p97 can exhibit this unfoldase/segregase using intrinsic ATPase (36–39). A previous study on RHBDL4 and p97 suggests that their direct interaction involves ERAD (13). In contrast, the RHBDL4 system we observed here was activating the substrate function of SREBP-1c like Nrf1 (40), implicating the p97-RHBDL4-SREBP-1c pathway as a reactive oxygen species (ROS) countermeasure. As supporting evidence for the involvement of p97 in this context, a p97 mutation knock-in ameliorated hepatosteatosis on high-fat fed mice due to impaired SREBP-1c activation (41). Current findings on SREBP-1 as a new RHBDL4 target also suggest that RHBDL4 can cleave type II membrane proteins along with previous known targets of type I. A low stringency of the recognition involves necessity for further topological exploration of this family.

That the protease activity of RHBDL4 varies according to the presence of different fatty acids highlights its role as a potential sensor of fatty acid saturation or possibly a sensor of the composition of the ER membrane. RHBDL4 cleavage activity on SREBP-1c was down-regulated by MUFA and PUFA but up-regulated in the presence of a relatively high amount of SFA. This provides an explanation for the long known regulation of SREBP-1c by UFA.

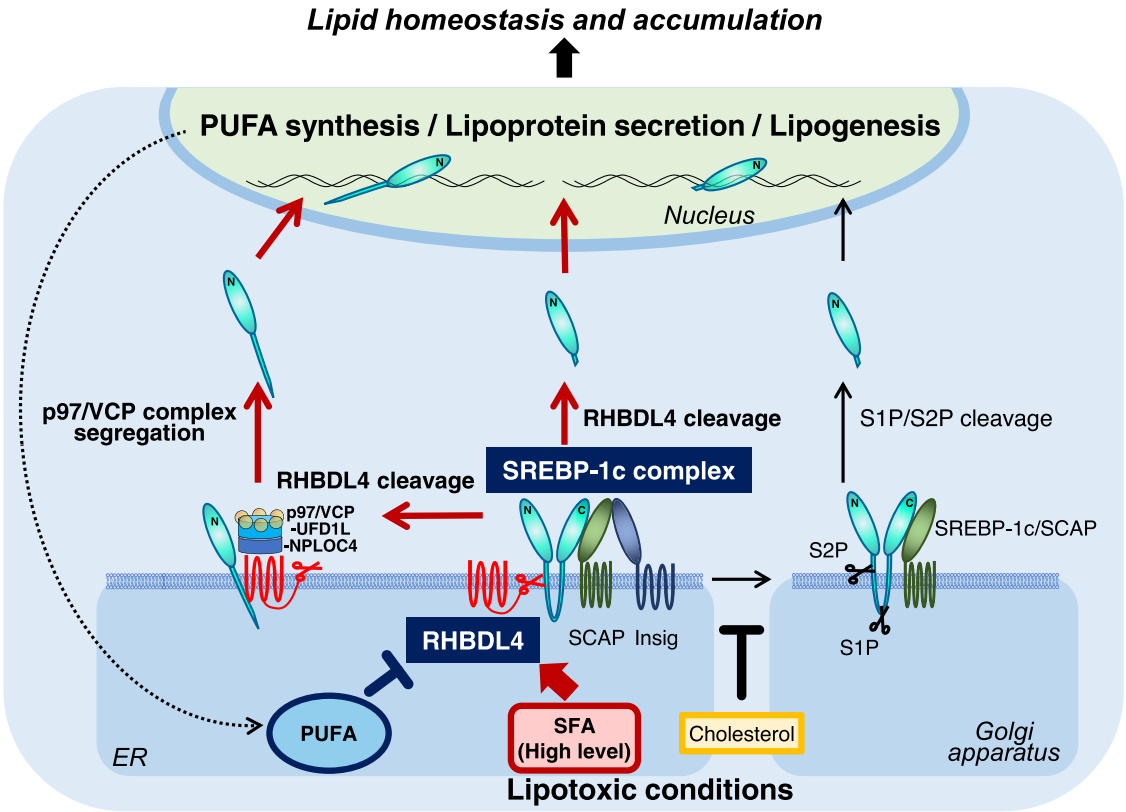

Fig. 7. Schematic representation of the novel activation mechanism of SREBP-1c by the RHBDL4 and p97 complex.

However, clear trends that were dependent on fatty acid chain length or degree of unsaturation did not emerge (Fig. S5C and D). As a novel membrane protease feature of a rhomboid family conferred by membrane immersion, intrinsic transmembrane segment dynamics of the rhomboid–substrate complex are thought to be important depending upon saturation of membrane fatty acids (42). Accordingly, our data imply that the RHBDL4-SREBP-1c interaction is preferable in the context of high SFA over PUFA and potentially relies on the ER membrane to form stable TM helices. It also needs to test the possibility of RHBDL4 as a direct acceptor or sensor for fatty acids. Further studies are needed to establish structure–function relationships. Taken together with knowledge of the unique features of rhomboid family proteins in possessing a high efficiency at lateral diffusion (43), the current findings of RHBDL4 sensing SFA/UFA make it tempting to speculate that potential allostatic responses to the RHBDL4-SREBP-1c pathway may be linked to the regulation of ER membrane fluidity.

The bona fide function of mammalian SREBP-1c has been recognized as regulating lipogenesis: the production of fatty acids and TGs for the supply of membrane lipids and energy storage, independent or dependent on cellular cholesterol levels. The current data in this study support RHBDL4 is a protease regulating this conventional role of SREBP-1c. Furthermore, RHBDL4 is deeply involved in regulation of PUFA metabolism (transport, synthesis, uptake, and remodeling of phospholipids) in the cell membrane. Taken together with the reciprocal regulation by PUFA and SFA, RHBDL4 might be a sensing and effector of fine-tuning machinery to monitor and maintain fatty acid composition in the ER membrane along with lipogenesis (Figs. 3F and 7). In addition, according to the gene expression profile from of RHBDL4 KO mice, RHBDL4 seems to regulate ER stress-related genes. From a pathophysiological standpoint, ω3 PUFAs possess antilipotoxicity and anti-inflammatory actions, protecting from fatty liver, insulin resistance, and anti-inflammatory action. The RHBDL4-SREBP-1c pathway could contribute to protect from the external stress by excessive SFA and cholesterol intakes and various inflammatory stimuli.

RNA-seq ontology analysis of RHBDL4 KO mice indicated that the substrate cleavage ability by RHBDL4 is related to cellular responses to hypoxia, ROS, monocyte inflammation, and fibrosis in addition to ER stress. We speculate that these regulations may be mediated by ER membrane fatty acid unsaturation both through SREBP-1-dependent and SREBP-1-independent pathways through other substrates of RHBDL4. While RHBDL4 absence suppressed SREBP-1c-mediated lipogenesis and hepatosteatosis on a short-term WD, we are currently evaluating chronic phenotypes of RHBDL4 KO mice after long WD feeding to ascertain its pathological and clinical relevance. In the future, it will be needed to evaluate the role of RHBDL4 for lipid metabolism independent on SREBP-1c.

Materials and methods

Mice

Eight-week-old male C57BL/6J (WT) mice were obtained from CLEA Japan. For WD analysis, 8-week-old male mice were fed for 14 days and sacrificed in a fed state. The WD consisted of 21% fat, 20% protein, and 50% carbohydrates (Research Diets, D12079B). For EPA-E treatment experiments, mice were fed on a WD for 14 days and treated with 5% EPA-E once a last day. For high-sucrose diet (HS) analysis, 8-week-old male mice were fed for 7 days and sacrificed in a fed state. HS consisted of 70% sucrose, 10% starch, and 20% casein supplemented with

methionine, vitamins, and minerals (Oriental Yeast). For 0.1% lovastatin and 0.025% ezetimibe (S/E) analysis, 8-week-old male mice were fed for 7 days and sacrificed in a fed state. All animal husbandry procedures and animal experiments were performed in accordance with the Regulation of Animal Experiments of the University of Tsukuba and were approved by the Animal Experiment Committee, University of Tsukuba.

RHBDL4 KO mice

Generation of RHBDL4 KO mice using a CRISPR/Cas9 system: The px330 vector (Addgene plasmid 42230) was a gift from Dr. Feng Zhang (44). The construct including green fluorescent protein (GFP)-stop codon was inserted at the end of Exon1 of the *Rhbdl4* (*Rhbdd1*) gene, generating RHBDL4 KO. RHBDL4 CRISPR F (5′-caccGTGTATGTGTGCCATAGCACAGG-3′) and RHBDL4 CRISPR R (5′-aaacCCTGTGCTATGGCACACATACAC-3′) oligo DNAs were annealed using standard methods. Annealed DNA was purified by ethanol precipitation. Short double-stranded DNA fragments were inserted into the BbsI restriction site of the px330 vector. The constructed plasmid was designated px330-RHBDL4. Female C57BL/6J mice were injected with one shot of pregnant mare serum gonadotropin and one shot of human chorionic gonadotropin at 48 h between injections and mated with male C57BL/6J mice. Fertilized one-cell embryos were collected from oviducts. Then, 5 ng/μL of px330 vector (circular) and 10 ng/μL dsDNA donors were injected into the pronuclei of one-cell-stage embryos according to standard protocols (45). Injected one-cell embryos were then transferred into pseudopregnant Institute of Cancer Research (ICR) mice.

In vitro cleavage assay

Recombinant HSV-human SREBP-1c-HA, human RHBDL4-V5, and RHBDL4 S144A-V5 proteins were prepared using a wheat germ cell-free protein synthesis system with liposomes (CFS) as described previously (46). Proteins were purified using HA and V5-magnetic beads (MBL), respectively, and subjected to an in vitro cleavage assay as described previously (12). Briefly, purified proteins were reacted in 50 mM Tris-HCl (pH 7.5), 150 mM NaCl, and 0.25% n-dodecyl-beta-D-maltoside (DDM) buffer for 2 h at 37°C and analyzed by SDS–PAGE and WB analysis (46).

Adenoviral overexpression of RHBDL4

For preparation of recombinant adenovirus, Myc-mouse RHBDL4 and GFP were subcloned into pENTR4 vectors (Invitrogen). Recombinant adenovirus plasmids were homologously recombined with pAd/CMV/V5-DEST vectors (Invitrogen), as per manufacturer's protocols. Recombinant adenoviruses were produced in HEK293A cells (Invitrogen) and purified by CsCl gradient centrifugation, as described previously (47). For adenovirus infection, mice were i.v. injected with adenovirus at a total dose of 5×10^{10} OPU/mouse; total infection amounts of adenovirus were adjusted using GFP adenovirus (47). Six days after infection, fasting and refeeding experiments were performed as described previously (48).

Histological analysis and metabolic measurements

Mouse livers were fixed, embedded in paraffin, sectioned, and stained with H&E. For ORO staining, liver tissues were harvested in cold phosphate buffered saline (PBS), fixed overnight at 4°C in 4% paraformaldehyde in PBS, cryoprotected in 30% sucrose in PBS, embedded in optimal cutting temperature compound (Sakura Finetek Inc.), and frozen. Frozen tissues were cut into 15-μm-thick cryosections and stained with ORO (Sigma-Aldrich). Plasma and liver parameters were measured as described previously (47). Fatty acid composition by gas chromatography was measured as described previously (28).

Acknowledgments

We are grateful to Drs. Makoto Shimizu, Ken Ebihara, and Daisuke Hishikawa and Prof. Takao Shimizu for their helpful discussion and Prof. Toni Vidal-Puig for critical reading of the manuscript. We also thank Kae Kumagai, Katsuko Okubo, Chizuko Fukui, Kenta Takei, Aoi Satoh, and Takuya Kikuchi for technical assistance and the members of our laboratories for discussion and helpful comments on the manuscript. The authors would like to thank Enago (www.enago.jp) for the English language review.

Supplementary Material

Supplementary material is available at *PNAS Nexus* online.

Funding

This work was supported by Grants-in-Aid for Scientific Research on Innovative Areas program (Inflammation Cellular Sociology) JP17H06395 (to H.S.), Scientific Research (A) 15H02541 and 18H04051 (to H.S.), and Scientific Research (C) 16K01811 and 19K11737 (to S.-I.H.) from the Ministry of Science, Education, Culture, and Technology of Japan; AMED-CREST Grant Number 16gm0910003h0002 (to H.S.) from the Japan Agency for Medical Research and Development, AMED; and Ono Medical Research Foundation (to S.-I.H.).

Author Contributions

S.-I.H., M.N., Y.N., and Hit.S. designed the experiments and wrote the manuscript. S.-I.H., M.N., Y.W., and M.A. performed the experiments. Y.Y. and Hiroa.T. performed computer simulation of RHBDL4–SREBP-1c complex. S.-I.H. and M.N. analyzed and interpreted the data. Hiroy.T., Yuh.M., K.M., H.O., K.K., Yuk.M., Y.A., Y.T., Y.O., Takaf.M., M.S., Takas.M., N.Y., Hir.S., H.D., R.S., and H.K. were involved in project planning and the discussion.

Preprint

This manuscript was posted on a preprint: https://doi.org/10.1101/2021.08.24.457590.

Data Availability

All study data are included in the article and/or supplementary material. RNA-seq data generated during this study are available at DNA Data Bank of Japan (DDBJ) database: DRA012520.

References

1 Horton JD, Goldstein JL, Brown MS. 2002. SREBPs: activators of the complete program of cholesterol and fatty acid synthesis in the liver. *J Clin Invest*. 109:1125–1131.
2 Shimano H, Sato R. 2017. SREBP-regulated lipid metabolism: convergent physiology—divergent pathophysiology. *Nat Rev Endocrinol*. 13:710–730.

3 Shimano H, *et al.* 1997. Isoform 1c of sterol regulatory element binding protein is less active than isoform 1a in livers of transgenic mice and in cultured cells. *J Clin Invest*. 99:846–854.
4 Horton JD, *et al.* 1998. Activation of cholesterol synthesis in preference to fatty acid synthesis in liver and adipose tissue of transgenic mice overproducing sterol regulatory element-binding protein-2. *J Clin Invest*. 101:2331–2339.
5 Shimomura I, Shimano H, Horton JD, Goldstein JL, Brown MS. 1997. Differential expression of exons 1a and 1c in mRNAs for sterol regulatory element binding protein-1 in human and mouse organs and cultured cells. *J Clin Invest*. 99:838–845.
6 Brown MS, Goldstein JL. 1999. A proteolytic pathway that controls the cholesterol content of membranes, cells, and blood. *Proc Natl Acad Sci U S A*. 96:11041–11048.
7 Jeon TI, Osborne TF. 2012. SREBPs: metabolic integrators in physiology and metabolism. *Trends Endocrinol Metab*. 23:65–72.
8 Yahagi N, *et al.* 1999. A crucial role of sterol regulatory element-binding protein-1 in the regulation of lipogenic gene expression by polyunsaturated fatty acids. *J Biol Chem*. 274:35840–35844.
9 Nakakuki M, *et al.* 2014. A novel processing system of sterol regulatory element-binding protein-1c regulated by polyunsaturated fatty acid. *J Biochem*. 155:301–313.
10 Lemberg MK. 2011. Intramembrane proteolysis in regulated protein trafficking. *Traffic*. 12:1109–1118.
11 Bergbold N, Lemberg MK. 2013. Emerging role of rhomboid family proteins in mammalian biology and disease. *Biochim Biophys Acta*. 1828:2840–2848.
12 Urban S, Wolfe MS. 2005. Reconstitution of intramembrane proteolysis in vitro reveals that pure rhomboid is sufficient for catalysis and specificity. *Proc Natl Acad Sci U S A*. 102:1883–1888.
13 Fleig L, *et al.* 2012. Ubiquitin-dependent intramembrane rhomboid protease promotes ERAD of membrane proteins. *Mol Cell*. 47:558–569.
14 Wunderle L, *et al.* 2016. Rhomboid intramembrane protease RHBDL4 triggers ER-export and non-canonical secretion of membrane-anchored TGFalpha. *Sci Rep*. 6:27342.
15 Strisovsky K, Sharpe HJ, Freeman M. 2009. Sequence-specific intramembrane proteolysis: identification of a recognition motif in rhomboid substrates. *Mol Cell*. 36:1048–1059.
16 Miao J, *et al.* 2014. Hepatic insulin receptor deficiency impairs the SREBP-2 response to feeding and statins. *J Lipid Res*. 55:659–667.
17 Bennett MK, Seo YK, Datta S, Shin DJ, Osborne TF. 2008. Selective binding of sterol regulatory element-binding protein isoforms and co-regulatory proteins to promoters for lipid metabolic genes in liver. *J Biol Chem*. 283:15628–15637.
18 VerHague MA, Cheng D, Weinberg RB, Shelness GS. 2013. Apolipoprotein A-IV expression in mouse liver enhances triglyceride secretion and reduces hepatic lipid content by promoting very low density lipoprotein particle expansion. *Arterioscler Thromb Vasc Biol*. 33:2501–2508.
19 Hashidate-Yoshida T, *et al.* 2015. Fatty acid remodeling by LPCAT3 enriches arachidonate in phospholipid membranes and regulates triglyceride transport. *eLife* 4:e06328.
20 Pauter AM, *et al.* 2014. Elovl2 ablation demonstrates that systemic DHA is endogenously produced and is essential for lipid homeostasis in mice. *J Lipid Res*. 55:718–728.
21 Moon YA, Hammer RE, Horton JD. 2009. Deletion of ELOVL5 leads to fatty liver through activation of SREBP-1c in mice. *J Lipid Res*. 50:412–423.
22 Varin A, *et al.* 2015. Liver X receptor activation promotes polyunsaturated fatty acid synthesis in macrophages: relevance in the context of atherosclerosis. *Arterioscler Thromb Vasc Biol*. 35: 1357–1365.
23 Rong X, *et al.* 2017. ER phospholipid composition modulates lipogenesis during feeding and in obesity. *J Clin Invest*. 127:3640–3651.
24 Hishikawa D, *et al.* 2020. Hepatic levels of DHA-containing phospholipids instruct SREBP1-mediated synthesis and systemic delivery of polyunsaturated fatty acids. *iScience* 23:101495.
25 Nguyen LN, *et al.* 2014. Mfsd2a is a transporter for the essential omega-3 fatty acid docosahexaenoic acid. *Nature* 509:503–506.
26 Ben-Zvi A, *et al.* 2014. Mfsd2a is critical for the formation and function of the blood-brain barrier. *Nature* 509:507–511.
27 Chan JP, *et al.* 2018. The lysolipid transporter Mfsd2a regulates lipogenesis in the developing brain. *PLoS Biol*. 16:e2006443.
28 Sekiya M, *et al.* 2003. Polyunsaturated fatty acids ameliorate hepatic steatosis in obese mice by SREBP-1 suppression. *Hepatology* 38:1529–1539.
29 Sato A, *et al.* 2010. Antiobesity effect of eicosapentaenoic acid in high-fat/high-sucrose diet-induced obesity: importance of hepatic lipogenesis. *Diabetes* 59:2495–2504.
30 Rape M, *et al.* 2001. Mobilization of processed, membrane-tethered SPT23 transcription factor by CDC48(UFD1/NPL4), a ubiquitin-selective chaperone. *Cell* 107:667–677.
31 Greenblatt EJ, Olzmann JA, Kopito RR. 2012. Making the cut: intramembrane cleavage by a rhomboid protease promotes ERAD. *Nat Struct Mol Biol*. 19:979–981.
32 Lee JN, Zhang X, Feramisco JD, Gong Y, Ye J. 2008. Unsaturated fatty acids inhibit proteasomal degradation of Insig-1 at a postubiquitination step. *J Biol Chem*. 283:33772–33783.
33 Olzmann JA, Richter CM, Kopito RR. 2013. Spatial regulation of UBXD8 and p97/VCP controls ATGL-mediated lipid droplet turnover. *Proc Natl Acad Sci U S A*. 110:1345–1350.
34 Kim J, *et al.* 2015. Identification of Rbd2 as a candidate protease for sterol regulatory element binding protein (SREBP) cleavage in fission yeast. *Biochem Biophys Res Commun*. 468:606–610.
35 Hwang J, *et al.* 2016. A Golgi rhomboid protease Rbd2 recruits Cdc48 to cleave yeast SREBP. *EMBO J*. 35:2332–2349.
36 Xia D, Tang WK, Ye Y. 2016. Structure and function of the AAA+ ATPase p97/Cdc48p. *Gene* 583:64–77.
37 Blythe EE, Olson KC, Chau V, Deshaies RJ. 2017. Ubiquitin- and ATP-dependent unfoldase activity of P97/VCP*NPLOC4*UFD1L is enhanced by a mutation that causes multisystem proteinopathy. *Proc Natl Acad Sci U S A*. 114:E4380–E4388.
38 Torrecilla I, Oehler J, Ramadan K. 2017. The role of ubiquitin-dependent segregase p97 (VCP or Cdc48) in chromatin dynamics after DNA double strand breaks. *Philos Trans R Soc Lond B Biol Sci*. 372:20160282.
39 Singh AN, *et al.* 2019. The p97-ataxin 3 complex regulates homeostasis of the DNA damage response E3 ubiquitin ligase RNF8. *EMBO J*. 38:e102361.
40 Radhakrishnan SK, den Besten W, Deshaies RJ. 2014. p97-dependent retrotranslocation and proteolytic processing govern formation of active Nrf1 upon proteasome inhibition. *eLife* 3:e01856.
41 Shibuya K, *et al.* 2022. AAA-ATPase valosin-containing protein binds the transcription factor SREBP1 and promotes its proteolytic activation by rhomboid protease RHBDL4. *J Biol Chem*. 298: 101936.
42 Moin SM, Urban S. 2012. Membrane immersion allows rhomboid proteases to achieve specificity by reading transmembrane segment dynamics. *eLife* 1:e00173.

43 Kreutzberger AJB, Ji M, Aaron J, Mihaljevic L, Urban S. 2019. Rhomboid distorts lipids to break the viscosity-imposed speed limit of membrane diffusion. *Science* 363:eaao0076.
44 Cong L, *et al.* 2013. Multiplex genome engineering using CRISPR/Cas systems. *Science* 339:819–823.
45 Gordon JW, Ruddle FH. 1981. Integration and stable germ line transmission of genes injected into mouse pronuclei. *Science* 214:1244–1246.
46 Takeda H, *et al.* 2015. Production of monoclonal antibodies against GPCR using cell-free synthesized GPCR antigen and biotinylated liposome-based interaction assay. *Sci Rep*. 5:11333.
47 Nakagawa Y, *et al.* 2006. TFE3 transcriptionally activates hepatic IRS-2, participates in insulin signaling and ameliorates diabetes. *Nat Med*. 12:107–113.
48 Ide T, *et al.* 2004. SREBPs suppress IRS-2-mediated insulin signalling in the liver. *Nat Cell Biol*. 6:351–357.